Journal of Natural Products
Vol. 58, No. 9, pp. 1392-1397, September 1995

IDENTIFICATION OF AN *N*-ACETYL KETO DERIVATIVE OF FUMONISIN B_1 IN CORN CULTURES OF *FUSARIUM PROLIFERATUM*

STEVEN M. MUSSER,* ROBERT M. EPPLEY, EUGENE P. MAZZOLA,

Center for Food Safety and Applied Nutrition, Food and Drug Administration, Washington, DC 20204

CHAD E. HADDEN, JOHN P. SHOCKCOR, RONALD C. CROUCH, and GARY E. MARTIN

Bioanalytical Sciences, Wellcome Research Laboratories, Research Triangle Park, North Carolina 27709

ABSTRACT.—A method is presented for the separation and identification of a new *N*-acetyl keto derivative of fumonisin B_1 (FB_1) produced in solid corn culture. Cultures of *Fusarium proliferatum* (M-1597) were purified using preparative hplc, and the new fumonisin was detected by negative-ion esms. Structures were confirmed by ^1H- and ^{13}C-nmr spectroscopy. The new fumonisin differs from FB_1 in that the tricarballylic acid functionality at the C-15 position of the eicosane backbone is replaced by a ketone and the amino group is acetylated. Direct analysis of the culture material by negative-ion electrospray lc/ms confirmed that the new fumonisin is produced naturally by the fungus.

Recent analysis of the secondary metabolites of *Fusarium moniliforme* has identified a new class of mycotoxins known as the fumonisins (1). Although the fumonisins have been identified in many species of *Fusaria* (2), several species, most notably *F. moniliforme* and *F. proliferatum,* are prolific producers of these toxins (3). Fumonisin B_1 (FB_1) [**1**] has been linked to equine leukoencephalomalacia (4), porcine pulmonary edema (5), and hepatotoxicity and carcinogenicity in rats (6). In addition to the animal toxicity of fumonisin, it is also suspected of being a causative agent in human esophageal cancer (7). Although FB_1 is the most abundant fumonisin produced by many species of *Fusaria*, several other structurally similar compounds have been identified (1, 8, 9). While the B series of fumonisins (B_1, B_2, and B_3) have been characterized rigorously, questions have arisen about the natural occurrence of the A series of fumonisins (*N*-acetyl amides of the B series) (10,11). Because HOAc is commonly used in the isolation procedure for the fumonisins, the possibility exists that the amide forms are simply by-products of the cleanup procedure. In this paper we report the identification of a new *N*-acetyl keto form of fumonisin, fumonisin AK_1 (FAK_1) [**2**], obtained directly from solid culture media.

RESULTS AND DISCUSSION

Compound **2** was isolated from extracts obtained from cultures of *F. proliferatum* by prep. hplc and analytical hplc. This procedure yielded approximately 600 μg of

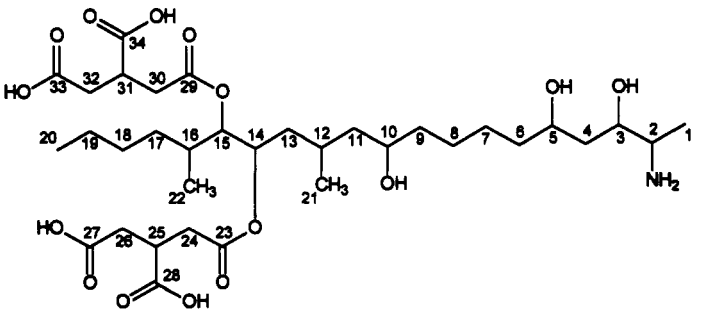

1

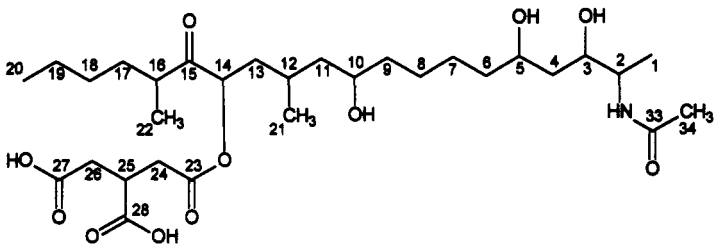

2

compound **2**, which was characterized by negative-ion esms and ^{1}H- and ^{13}C-nmr spectroscopy. A mol wt of 603 daltons was determined for compound **2**. The negative-ion ms of **2** showed only a molecular anion at *m/z* 602 with no observed fragmentation. This compound was originally suspected to be the *N*-acetyl amide of **1** in which one of the tricarballylic acid side-chains had been hydrolyzed. However, the observed mol wt, which was not correct for that compound, instead suggested a degree of unsaturation in addition to the loss of one of the tricarballylic acid side-chains. Attempts to locate the position of unsaturation by ms techniques were unsuccessful.

Analysis of approximately equimolar amounts of **1** and **2**, using positive-ion electrospray conditions, showed the signal for **2** to be approximately 25% of the signal observed for **1**. This finding indicates that the amine present in **2** is functionalized in such a way as to make protonation difficult, consistent with *N*-acetylation. If **2** were an *O*-acetyl derivative of **1**, the response would be expected to be at or near that of **1** in positive-ion esms, not suppressed as is the case for amides. Direct analysis of an extract from culture material of *F. proliferatum* by negative-ion electrospray lc/ms clearly showed the presence of compound **2**. Because this material was not subject to any pre-treatment, the ms analysis confirmed that **2** occurs naturally and is not a by-product of the preparative-scale procedure.

^{1}H-^{1}H COSY, direct ^{1}H-^{13}C HMQC, and indirect ^{1}H-^{13}C (HMBC and HMQC-TOCSY) 2D nmr experiments were crucial to the structural elucidation and spectral assignment of **2**. COSY and HMQC-TOCSY spectra permitted the establishment of the complete proton spin-coupling network of the eicosane backbone from C-1–C-20 (Table 1). Especially important, however, was the subsystem comprising those protons from the C-20-methyl group (which are the only protons to appear as a triplet) through H-16 and the C-22-methyl group at 2.78 and 1.01 ppm, respectively. The latter methyl group displayed a strong three-bond connectivity to the ketone carbonyl resonance at 219 ppm in the HMBC spectrum, which thus placed the ketone functionality at the 15-position and not the 14-position. In addition, COSY spectra placed the most deshielded proton (carbinol ester) at C-14, which confirmed the presence of the tricarballylic acid functionality at that position and not at C-15. Finally, the comparative overnight direct observe ^{13}C-nmr spectra shown in Figure 1 were acquired for **2** in 40 μl of D_2O, using a Varian heteronuclear Nano-probe™, and in 120 μl of D_2O using a Nalorac Z•SPEC® MC-500-3 carbon-optimized micro-probe.

The utilization of micro- and nano-probe technologies to elucidate the structure of **2** and to assign totally the ^{1}H- and ^{13}C-nmr spectra with a sample consisting of ca. 0.3 μmol illustrates the improvement in sensitivity afforded by improvements in probe design. The enhanced capabilities offered by micro-/nano-detection techniques offer considerable promise for the elucidation of complex natural product structures which have heretofore been inaccessible because of the stringently limited availability of samples.

TABLE 1. ^{1}H- and ^{13}C-Nmr Data for **2**.[a]

Position	δ_H[b] (*J*)	δ_C[c]	n_H	Position	δ_H[b] (*J*)	δ_C[c]	n_H
1	1.0 d (7)	18.4	3	17	1.48	33.9	2
2	3.72	52.3	1		1.23		
3	3.66 dt (9,2)	72.5	1	18	1.08	31.3	2
4	1.4 m	42.1	2		1.02		
5	3.70	70.3	1	19	1.16	24.4	2
6	1.42	39.2	2		1.14		
	1.38			20	0.72 t (7)	15.6	3
7	1.28 m	27.1	2	21	0.85 d (7)	21.6	3
8	1.28 m	27.3	2	22	1.01 d (7)	19.7	3
9	1.28 m	27.1[d]	2	23	—	181.6	0
10	3.64	71.4	1	24	2.72 dd (17,7)	38.2	2
11	1.41	44.6	2		2.57 m		
	1.17			25	3.00 dt (7)	41.4	1
12	1.74	28.6	1	26	2.59 m	39.3	2
13	1.65	39.0	2		2.42 dd (17,7)		
	1.49			27	—	179.9	0
14	5.18 dd (9,2)	79.4	1	28	—	176.2	0
15	—	219.5	0	33	—	175.9	0
16	2.78	44.8	1	34	1.86	24.5	3

[a]In D_2O.

[b]Relative to residual HDO at 4.62 ppm.

[c]Relative to dioxane at 67.4 ppm.

[d]Assignment based on HMQC spectrum and double-intensity ^{13}C-nmr signal recorded with the Nalorac micro-probe.

EXPERIMENTAL

GENERAL EXPERIMENTAL PROCEDURES.—A C_8 basic column, 2.0×250 mm (YMC, Inc., Greensboro, NC), was used for all separations with a constant flow rate of 200 μl/min. A gradient mobile phase separation as described below was used for all hplc analysis. The column effluent was split 10:1 such that 20 μl/min was diverted to the mass spectrometer and 180 μl/min was diverted to a uv detector (190 nm). Mass spectrometry was carried out on a quadrupole mass spectrometer (Finnigan Corp., San Jose, CA) controlled by a data system (Teknivent, Maryland Heights, MO). The mass spectrometer was fitted with an electrospray ion source (Vestec, Houston, TX) in which the needle had been modified for pneumatically assisted ionization (12). The needle voltage was −4 kV, the source temperature was 110°, and SF_6 was used as a nebulizer gas.

FUNGAL MATERIAL.—Cultures of *Fusarium proliferatum* (M-1597), grown on solid corn as previously described (2), were provided by P.E. Nelson of the Fusarium Research Center, Pennsylvania State University. Levels of production of **1** were approximately 3–5 mg/g of solid culture material.

EXTRACTION AND ISOLATION.—Solid culture material (500 g) was extracted with 2 liters of MeOH-H_2O (75:25) and filtered through a Buchner funnel (5 ml of this solution was freeze-dried and the solid was reserved for lc/ms analysis). The filtate was diluted with H_2O to a final MeOH concentration of 30%. The diluted solution was pumped at 20 ml/min onto a Bondapak C_{18} prep. chromatography column, 40×400 mm, 20 μm, 125 Å (Waters Corp.). The column was washed with H_2O for 80 min, then with MeOH-H_2O (50:50) for 20 min, and the fraction containing **1** and structurally related amides was eluted with MeOH-H_2O (70:30). The MeOH was removed under vacuum and the aqueous portion was applied to a Dynamax C_{18} column, 41.4×250 mm, 8 μm, 60 Å (Rainin Corp.), at a flow rate of 50 ml/min. The column was washed with a solution of MeCN-H_2O (25:75) for 50 min, and the fraction containing **1** and structurally related amides was eluted with MeCN-H_2O (70:30). The MeCN was removed under vacuum, and the aqueous solution was applied to a μBondapak cyano column, 40×400 mm, 10 μm, 125 Å (Waters Corp.), at a rate of 50 ml/min. Fumonisins were eluted with 1% pyridine in H_2O. The pyridine was removed by re-chromatographing the solution on the Bondapak C_{18} system. Compounds **1** and **2** were eluted with MeCN-H_2O (30:70). The eluate was collected and freeze-dried, yielding 2 g of solid material (approximately 93% **1**). The freeze-dried material was further fractionated on a C_8 basic column, 4.6×250 mm (YMC, Inc.), with a mobile phase flow rate of 1 ml/min. A MeCN gradient containing 0.1% HOAc (pH 3), beginning at

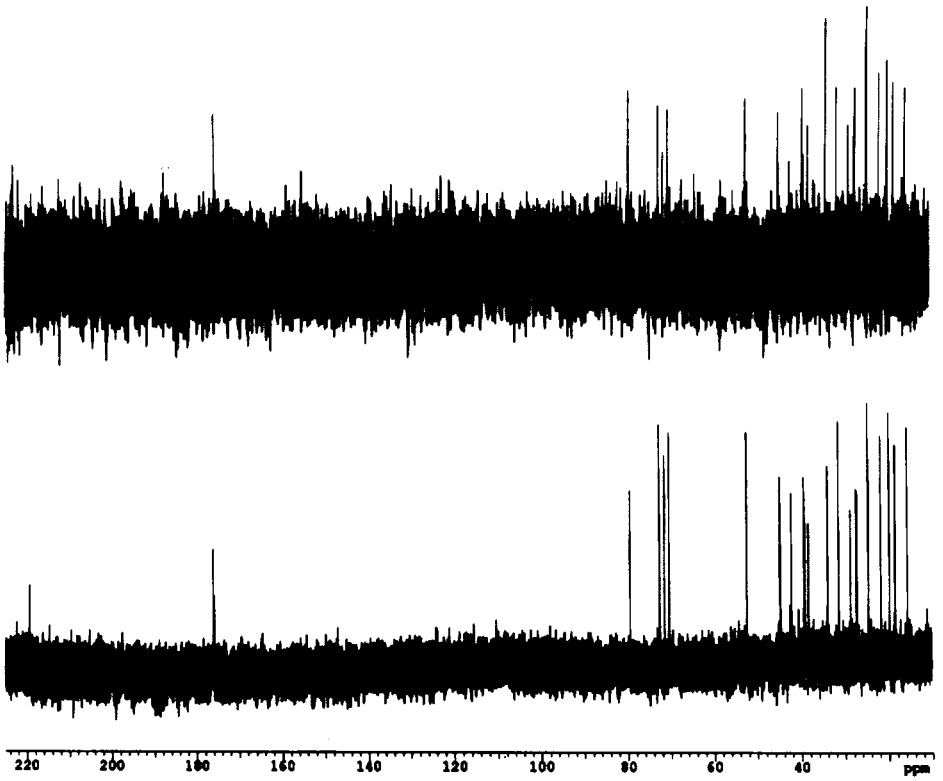

FIGURE 1. ^{13}C-Nmr spectra of approximately 200 μg of **2**. Top trace—overnight acquisition (22,528 transients) obtained using a Nalorac Z•SPEC® MC-500-3 carbon-optimized micro-probe (s/n=5.5:1). Bottom trace—overnight acquisition (26,800 transients) obtained using a Varian heteronuclear Nano-probe™ with the sample dissolved in 40 μl of D_2O (s/n=11:1).

MeCN-H_2O (20:80) and changing linearly to MeCN-H_2O (45:55) in 35 min, was used to separate **2** from **1**. The collected fractions were freeze-dried, yielding 600 μg of **2**.

NUCLEAR MAGNETIC RESONANCE SPECTROSCOPY.—The ^{1}H-nmr and ^{13}C-nmr spectra of **2** were recorded on Varian Unity 400 and Unity 500 spectrometers. The Unity 400 was equipped with Nalorac Z•SPEC® MID-400-3 micro inverse-detection and MD-400-3 micro dual probes. The Unity 500 was equipped with Nalorac Z•SPEC® MID-500-3 micro inverse-detection and MC-500-3 carbon-optimized micro-probes. A Varian heteronuclear Nano-probe™ was also used with the 500 MHz instrument. All spectra were acquired using a test solution consisting of 200 μg of **2** dissolved in 120 μl of D_2O; proton chemical shifts were referenced to the residual H_2O resonance at 4.62 ppm. The proton spectral width was 2762.6 Hz. The data were acquired using a 11.3-μsec pulse (90°-pulse width=17 μsec). A total of 32 transients provided an adequate signal-to-noise ratio (s/n) for the proton reference spectrum.

The ^{13}C-nmr reference spectra were recorded using both a Nalorac Z•SPEC® MC-500-3 carbon-optimized micro probe and a Varian heteronuclear Nano-probe™. The former data were acquired from the 120-μl test solution used for the inverse-detection experiments; the latter were obtained after all other spectral data were acquired. For ^{13}C-nmr spectral acquisition with the Nalorac micro-probe, the data were acquired by using a 5.4-μsec pulse (60° pulse; 90° pulse length=8.1 μsec at tpwr=55) and a 0.788-sec interpulse delay. The spectral width was 27,045 Hz (215 ppm) with the transmitter positioned to include the carbonyl resonance; the spectrum was digitized with 64K data points giving an acquisition time of 1.212 sec. A total of 22,528 transients was accumulated to give s/n=5.5:1 (see top trace, Figure 1). The ^{13}C-nmr spectrum recorded using the nano-probe was acquired after the volume of the test solution was reduced from 120 to 20 μl, which was transferred to a 40-μl nano-cell. The vial was rinsed with two 10-μl portions of D_2O to ensure quantitative transfer to the nano-cell. The data were acquired using a 4.9-μsec pulse (60° pulse; the 90°-pulse width was 7.4 μsec at tpwr=55). All other spectral parameters were identical to those

used with the micro-probe. The spin rate was 2.5 KHz. Altogether, 26,880 transients were accumulated to afford the spectrum shown as the bottom trace in Figure 1, which gave s/n=11:1. Hence, while the overnight performance of the nano-probe was better than that of the micro-probe, it was less than would have been expected from the relative differences in the concentrations used in the acquisition of the two spectra.

The 500-MHz COSY spectrum of **2** was acquired as 1536×320 files with 32 transients accumulated per file and a 1.197-sec interpulse delay. The data were processed by using sinebell multiplication prior to both Fourier transforms with zero filling to give a final data matrix of 1K×1K points, which were symmetrized before plotting.

The inverse-detected HMQC spectrum of **2** was acquired using the pulse sequence of Bax and Subramanian (13) modified for States TPPI acquisition of the data (14). The data were acquired at 400 MHz at 1024×(96×2) hypercomplex files; altogether 112 transients were accumulated per file with an interpulse delay of 1.24 sec. Spectral widths were 2249 and 8046 Hz in F_2 and F_1, respectively, giving acquisition times of 0.228 and 0.005 sec, respectively. Pulse widths were 8.8 μsec at tpwr=57 for the 90° ^{1}H pulse and 11.5 μsec at 59 for the 90° ^{13}C pulse from the X-decoupler. Delays optimized as a function of the one-bond heteronuclear coupling constant were optimized for an assumed coupling constant of 150 Hz. The data were processed using Gaussian multiplication prior to both Fourier transforms.

The HMQC-TOCSY spectrum (15) of **2** was acquired at 500 MHz using the IDR-HMQC-TOCSY modification of Martin *et al.* (16) with a (-Δ-180° ^{1}H/180° ^{13}C-Δ-) pulse sandwich following the isotropic mixing period to invert the direct responses after the method of Domke (17). The data were acquired as 1024×(128×2) hypercomplex files using the States TPPI modification as in the HMQC experiment. A 1.5-sec interpulse delay was used between acquisitions; the H_2O resonance was saturated during the interpulse delay with low power on-resonance decoupling. The data were processed using Gaussian multiplication prior to both Fourier transforms with zero filling to give a final matrix of 2048×512 points. The spectral widths were 2762 and 9428 Hz in F_2 and F_1, respectively, giving acquisition times of 0.185 and 0.006 sec, respectively. A total of 160 transients was accumulated per file. Delays based on the 1-bond heteronuclear coupling constant were optimized for an assumed coupling of 150 Hz. Pulse widths were 7.3 μsec at tpwr=61 for the 90° pulses and 25 μsec at 49 for the 90° pulse at the power level used for the MLEV-based isotropic mixing period (22 msec in duration and flanked by 2-msec trim pulses); 90° ^{13}C pulses from the X-decoupler were 12.0 μsec at a power of 63.

The long-range heteronuclear shift correlation spectrum (HMBC) was acquired at 500 MHz using the pulse sequence of Bax and Summers (18). Delays based on the long-range heteronuclear coupling were optimized for 63 msec (6 Hz); delays based on the 1-bond heteronuclear coupling were optimized for an assumed average one-bond coupling constant of 140 Hz. Altogether, 64 transients were accumulated per file. A 1.5-sec interpulse delay was used; the H_2O signal was saturated during the interpulse delay by low power on-resonance decoupling. The data were acquired as 2048×(256×2) hypercomplex files and were processed by a combination of Gaussian and shifted-Gaussian multiplication prior to the first Fourier transform and cosine multiplication prior to the second transform with zero filling to give a final data matrix consisting of 2048×1024 points. Spectral widths were 2762 and 26,774 Hz in F_2 and F_1, respectively, giving acquisition times of 0.371 and 0.014 sec, respectively. Pulse widths were identical to those reported for the IDR-HMQC-TOCSY experiment.

LITERATURE CITED

1. S.C. Bezuidenhout, W.C.A. Gelderblom, C.P. Gorst-Allman, R.M. Horak, W.F.O. Marasas, G. Spiteller, and R. Vleggaar, *J. Chem. Soc., Chem. Commun.*, 743 (1988).
2. P.E. Nelson, R.D. Plattner, D.D. Shackelford, and A.E. Desjardins, *Appl. Environ. Microbiol.*, **58**, 984 (1992).
3. P.F. Ross, P.E. Nelson, J.L. Richard, G.D. Osweiler, L.G. Rice, R.D. Plattner, and T.M. Wilson, *Appl. Environ. Microbiol.*, **56**, 3225 (1990).
4. W.F.O. Marasas, T.S. Kellerman, W.C.A. Gelderblom, J.A.W. Coetzer, P.G. Thiel, and J.J. Van der Lugt, *Onderstepoort J. Vet. Res.*, **55**, 197 (1988).
5. L.R. Harrison, B.M. Colvin, J.T. Greene, L.E. Newman, and J.R. Cole, *J. Vet. Diagn. Invest.*, **2**, 217 (1990).
6. W.C.A. Gelderblom, N.P.J. Kriek, W.F.O. Marasas, and P.G. Thiel, *Carcinogenesis*, **12**, 1247 (1991).
7. E.W. Sydenham, P.G. Thiel, W.F.O. Marasas, G.S. Shephard, D.J. Van Schalkwijk, and K.R. Koch, *J. Agric. Food Chem.*, **38**, 1900 (1990).
8. M.E. Cawood, W.C.A. Gelderblom, R. Vleggaar, Y. Behrend, P.G. Thiel, and W.F.O. Marasas, *J. Agric. Food Chem.*, **39**, 1958 (1991).
9. R.D. Plattner, D. Weisleder, D.D. Shackelford, R. Peterson, and R.G. Powell, *Mycopathologia*, **17**, 23 (1992).

10. B.E. Branham and R.D. Plattner, *J. Nat. Prod.*, **56**, 1630 (1993).
11. P.E. Nelson, A.E. Desjardins, and R.D. Plattner, *Ann. Rev. Phytopathol.*, **31**, 233 (1993).
12. M.G. Ikonomou, A.T. Bladesand, and P. Kebarle, *J. Am Soc. Mass Spectrom.*, **2**, 497 (1991).
13. A. Bax and S. Subramanian, *J. Magn. Reson.*, **67**, 565 (1986).
14. D. Marion, M. Ikura, R. Tschudin, and A. Bax, *J. Magn. Reson.*, **85**, 393 (1989).
15. L. Lerner and A. Bax, *J. Magn. Reson.*, **69**, 375 (1986).
16. G.E. Martin, T.D. Spitzer, R.C. Crouch, J.-K. Luo, and R.N. Castle, *J. Heterocyclic Chem.*, **29**, 577 (1992).
17. T. Domke, *J. Magn. Reson.*, **95**, 174 (1991).
18. A. Bax and M.F. Summers, *J. Am. Chem. Soc.*, **108**, 2093 (1986).

Received 9 January 1995